Noname manuscript No.
(will be inserted by the editor)

Concurrent topological optimization of two bodies sharing design space: problem formulation and numerical solution

First Author · Second Author

Received: date / Accepted: date

Abstract cite as: Previati, G., Ballo, F., Gobbi, M., "Concurrent topological optimization of two bodies sharing design space: problem formulation and numerical solution", Struct Multidisc Optim (2019) 59: 745. https://doi.org/10.1007/s00158-018-2097-x

Topology optimization is a widely used technique for deriving efficient structural layouts for components in many engineering fields. The optimization process deals with the definition of the optimal material distribution of single components subjected to specified loads and boundary conditions, in case made of different materials or with embedded regions corresponding to other components or actuators. In this paper, a novel topology optimization problem is proposed. The case

F. Author

first address

Tel.: +123-45-678910

Fax: +123-45-678910

E-mail: fauthor@example.com

S. Author

second address

of the concurrent topological optimization of two different components sharing a part of the design spaces is considered. The design problem represents a design situation in which more than one component has to be fitted in an enclosed space and each component has its own load carrying function.

In the paper, the problem is solved by a numerical technique able to allocate the common part of the design space to each component. Inside the allocated space, the actual material distribution of the component is optimized by a standard topological optimization algorithm. Numerical examples are provided to show the potentialities of the method. A (simplified) practical design problem is also considered.

Keywords Topological optimization · multi-domain optimization · multi-component optimization

1 Introduction

The topological optimization of engineering components is a well discussed topic. In the literature many papers and books can be found defining the basis of topological optimization and presenting states of the art and prospectives (see for instance Rozvany (2009); Guo and Cheng (2010); Eschenauer and Olhoff (2001); Bendsøe and Sigmund (2004); Zhu et al. (2016); Zhang et al. (2016a)). Many methods have been developed to face topology optimization problems, among them, the most used, especially in available software, is the SIMP method (Rozvany (2009)).

Classical problems of topology optimization involve the optimal design of single components (Bendsøe and Sigmund (2004)). For such kind of problems many examples and even free subroutines can be found (Sigmund (2001)). More recently,

multi-domain problems have been considered. An application of multi-domain optimization is the design of multi-phase or multi-material structures (Tavakoli and Mohseni (2014)). In this class of problems, a single component is designed taking into account that the component can be realized by using more than one material. Level set based approaches have been extensively used to solve such kind of problems (Mei and Wang (2004); Wang and Wang (2004); Luo et al. (2009)) and recently became very attractive for the optimal design of innovative mechanical metamaterials (Wang et al. (2017); Vogiatzis et al. (2017); Wang et al. (2016)).

The optimization of multi-component structures has been considered in some papers. In most cases (Zhang et al. (2012); Qian and Ananthasuresh (2004); Xia et al. (2013); Zhang et al. (2015)), the optimization refers to the definition of the optimal structural layout of a part of the structure in which are embedded rigid structures or voids that can change position or orientation during the optimization process but maintain their original geometries. In few cases, small changes in the embedded components are considered (Clausen et al. (2014)). Actuators can be embedded to obtain smart structures (Wang et al. (2014)).

Referring to the simultaneous optimization of two bodies, in case sharing part of the design domain, some applications of the level set method can be found. In Lawry and Maute (2018) and in Strömberg (2018), the focus is on the optimization of the interface between two, or more, phases (components) in order to obtain some prescribed interaction force. The solution of such problems involves also the division of the design space between the two components. In general, level set based approaches for multi-material problems have the potential to solve the simultaneous optimization of two bodies. In Zhang et al. (2016b) a completely

different approach, the Moving Morphable Components approach Zhang et al. (2016b), which seems to be adaptable to solve such problems is discussed.

The present paper aims to solve problems in which two different components share part of the design space in the framework of the Solid Isotropic Microstructure (or Material) with Penalization for intermediate densities (SIMP, Rozvany (2009)) approach. This kind of approach will guarantee a easy implementation of the proposed approach to three dimensional problems. A numerical algorithm based on the classical density-based approach for the optimal material distribution in a given design space and able to address the concurrent topological optimization is proposed. The algorithm will also consider the optimal allocation of material and voids inside a shared region of the design domains of the two bodies.

The algorithm will be tested in two- and three-dimensional frameworks in the simple case of two bodies sharing part of their design space but not interacting. A wheel and brake caliper assembly will be discussed as example in the last section of the paper. In this examples, the design domains of the caliper and the wheel occupy the same space and the optimal distribution of this space has to be found along with the optimal material distribution in the two components. Also, the example~~s~~ shows the possibility to use the proposed algorithm along with a commercial finite element software allowing for the solution of complex three dimensional problems.

The paper is organized as follows. In the next section (Sect. 2) the mathematical formulation of the problem will be given. Then, in Sect. 3, a numerical algorithm able to solve the concurrent optimization problem will be discussed. Finally, three examples will be provided in Sect. 4.

2 Problem formulation and numerical solution

In this section the design problem of the concurrent topological optimization of two bodies sharing a portion of the design space is stated.

In fig. 1 left, the generalized geometries of two bodies sharing (a portion of) the design space are depicted. The design domain of the two bodies are denominated Ω_1 and Ω_2. Ω_{1-2} represents the shared portion of the design space. The space of this region can be occupied by any of the two bodies. Of course, only one body at a time can occupy a given point in the region. The goal of the optimization procedure is to allocate in a convenient way the shared space (or leave it void) while, at the same time, optimizing the material distribution of the two bodies under the applied loads $\mathbf{f_1}$ and $\mathbf{f_2}$ and the given boundary constraints on Γ_1 and Γ_2.

It must be emphasized that the portion of the shared domain Ω_{1-2} to be allocated to each body is not given a priori, but must be allocated during the optimization process and can change according to the evolution of the material distributions of the two bodies themselves.

In the following, the problem will be addressed under the hypotheses of

- linear elastic bodies with small deformations;
- the two bodies do not interact in the shared portion of the domain (i.e. no contact is considered between the two bodies in the shared portion of the domain, interactions between the two bodies outside this region is possible);
- each body is made by only one isotropic material;
- both materials have the same reference density, but they can have different elastic moduli;

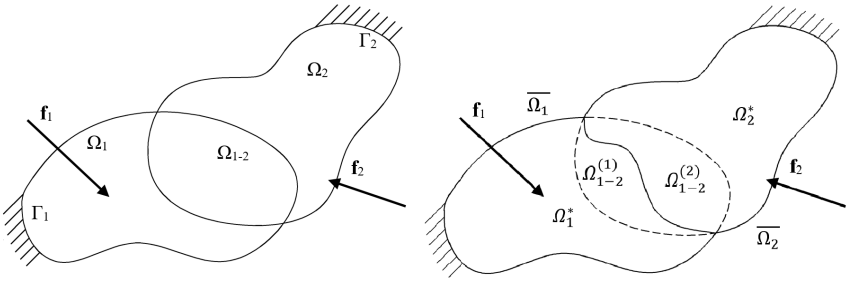

Fig. 1 Generalized geometries of the design domains (Ω_1 and Ω_2) of two bodies sharing a portion of the design space. Each body has its own system of applied forces ($\mathbf{f_1}$ and $\mathbf{f_2}$) and boundary constraints (Γ_1 and Γ_2). Ω_{1-2} represents the shared portion of the design space. Left: initial definition of the domains. Right: division of the domains with assignment of the shared portion of the design space to each body.

- loads and boundary conditions can be applied in any point of the domains, even in the shared portion;
- the structural problem is formulated by the finite element theory.

Let us call Ω_1^* and Ω_2^*, see Fig. 1 right, the two unshared parts of the domains Ω_1 and Ω_2 respectively (s.t. $\Omega_1 = \Omega_1^* + \Omega_{1-2}$ and $\Omega_1 = \Omega_1^* + \Omega_{1-2}$). The concurrent optimization problem can be stated as

$$
\begin{aligned}
&\textit{Find} \quad \min_{\mathbf{u_1},\mathbf{u_2},\rho} \left(l_1\left(\mathbf{u_1}\right) + l_2\left(\mathbf{u_2}\right)\right) \\
&\\
&\textit{s.t.}: \quad a_1\left(\mathbf{u_1},\mathbf{v_1}\right) = l_1\left(\mathbf{u_1}\right) \;\; \textit{and} \;\; a_2\left(\mathbf{u_2},\mathbf{v_1}\right) = l_1\left(\mathbf{u_2}\right) \;\; \forall \mathbf{v_1},\mathbf{v_2} \in U_1, U_2 \\
&\qquad E^1_{ijkl}\left(\mathbf{x_1}\right) = \rho\left(\mathbf{x_1}\right)^p E^{*1}_{ijkl}, \qquad \mathbf{x_1} \in \Omega^*_1 \cup \Omega^{(1)}_{1-2} = \overline{\Omega_1} \\
&\qquad E^2_{ijkl}\left(\mathbf{x_2}\right) = \rho\left(\mathbf{x_2}\right)^p E^{*2}_{ijkl}, \qquad \mathbf{x_2} \in \Omega^*_2 \cup \Omega^{(2)}_{1-2} = \overline{\Omega_2} \\
&\qquad \Omega^{(1)}_{1-2} \cup \Omega^{(2)}_{1-2} = \Omega_{1-2} \;\; \textit{and} \;\; \Omega^{(1)}_{1-2} \cap \Omega^{(2)}_{1-2} = \emptyset \\
&\qquad \textstyle\int_{\overline{\Omega_1}} \rho\left(\mathbf{x_1}\right) d\Omega + \int_{\overline{\Omega_2}} \rho\left(\mathbf{x_2}\right) d\Omega \leq V \qquad 0 \leq \rho \leq 1
\end{aligned}
\tag{1}
$$

$$
\begin{aligned}
&\textit{where}: l_1\left(\mathbf{u_1}\right) = \textstyle\int_{\overline{\Omega_1}} \mathbf{f_1}\mathbf{u_1} d\overline{\Omega_1} \;\; \textit{and} \;\; l_2\left(\mathbf{u_2}\right) = \int_{\overline{\Omega_2}} \mathbf{f_2}\mathbf{u_2} d\overline{\Omega_2} \\
&\qquad a_1\left(\mathbf{u_1},\mathbf{v_1}\right) = \textstyle\int_{\overline{\Omega_1}} E^1_{ijkl}\left(\mathbf{x_1}\right) \epsilon_{ij}\left(\mathbf{u_1}\right) \epsilon_{kl}\left(\mathbf{v_1}\right) d\Omega_1 \\
&\qquad a_2\left(\mathbf{u_2},\mathbf{v_2}\right) = \textstyle\int_{\overline{\Omega_2}} E^2_{ijkl}\left(\mathbf{x_2}\right) \epsilon_{ij}\left(\mathbf{u_2}\right) \epsilon_{kl}\left(\mathbf{v_2}\right) d\Omega_2 \\
&\qquad \overline{\Omega_1} \;\; \textit{and} \;\; \overline{\Omega_2} \;\; \textit{connected}
\end{aligned}
$$

Being l_1 and l_2 the compliance functions of the two bodies, a_1 and a_2 the internal virtual work functions of the two bodies, $\mathbf{u_1}$ and $\mathbf{u_2}$ the displacement fields, $\mathbf{v_1}$ and $\mathbf{v_2}$ the virtual displacement fields, $\mathbf{x_1}$ and $\mathbf{x_2}$ the points of the domains, $\mathbf{f_1}$ and $\mathbf{f_2}$ the applied loads, E^1_{ijkl} and E^2_{ijkl} the material stiffness tensors, E^{*1}_{ijkl} and E^{*2}_{ijkl} the stiffness tensors of the reference materials and ρ the pseudo-density.

In the problem stated in Eq. 1 the design variables are represented by the two pseudo-densities fields $\rho\left(\mathbf{x_1}\right)$ and $\rho\left(\mathbf{x_2}\right)$ and by the domain $\Omega^{(1)}_{1-2}$. In fact, in addition to the optimal material distribution inside the two domains, also the division of the common domain has to be found. Thus, domain $\Omega^{(1)}_{1-2}$ is a design variable in the sense that in the solution of the stated problem, each point of Ω_{1-2} has to be assigned either to $\Omega^{(1)}_{1-2}$ or $\Omega^{(2)}_{1-2}$. The domain $\Omega^{(2)}_{1-2}$ is not a design variable, as it is trivially given by $\Omega^{(2)}_{1-2} = \Omega_{1-2} \cap \Omega^{(1)}_{1-2}$.

The two domains $\overline{\Omega_1}$ and $\overline{\Omega_2}$ represent the regions where the two bodies are topologically optimized at any cycle of the optimization procedure. Each individual domain, i.e. $\overline{\Omega_1}$ and $\overline{\Omega_2}$, should consist of one geometrical region, without disconnected parts. This requirement ensures physically realizable solutions.

Given the formulation of the problem of Eq. 1, the reference stiffness E^{*1}_{ijkl} and E^{*2}_{ijkl} are multiplying parameters allowing the inclusion in the problem of different stiffness for the materials of the two bodies. The pseudo-density ρ is a design variable. In the considered formulation, the materials of the two bodies actually have the same reference density. Different densities could be included in the problem by a proper normalization procedure.

3 Numerical solution

For its numerical solution, the problem of Eq. 1 is written in a discretized form as

$$
\begin{aligned}
&Find \quad \min_{\mathbf{u_1},\mathbf{u_2},\rho} \left(\mathbf{f_1^T u_1} + \mathbf{f_2^T u_2}\right) \\
&s.t.: \quad \mathbf{K}\left(\mathbf{E_e^1}\right)\mathbf{u_1} = \mathbf{f_1} \;\; and \;\; \mathbf{K}\left(\mathbf{E_e^2}\right)\mathbf{u_2} = \mathbf{f_2} \\
&\qquad \mathbf{E_e^1} = \rho\left(\mathbf{x_e}\right)^p \mathbf{E_e^{*1}}, \qquad \mathbf{x_e} \in \overline{\Omega_1} \\
&\qquad \mathbf{E_e^2} = \rho\left(\mathbf{x_e}\right)^p \mathbf{E_e^{*2}}, \qquad \mathbf{x_e} \in \overline{\Omega_2} \\
&\qquad \Omega^{(1)}_{1-2} \cup \Omega^{(2)}_{1-2} = \Omega_{1-2} \;\; and \;\; \Omega^{(1)}_{1-2} \cap \Omega^{(2)}_{1-2} = \emptyset \\
&\qquad \sum_{e=1}^{N_1} \rho\left(\mathbf{x_e}\right) + \sum_{e=1}^{N_2} \rho\left(\mathbf{x_e}\right) \leq V \qquad 0 < \rho_{min} \leq \rho \leq 1 \\
&where: \; \mathbf{K}\left(\mathbf{E_e^1}\right) = \textstyle\sum_{e=1}^{N_1} \mathbf{K_e}\left(\mathbf{E_e^1}\right) \;\; and \;\; \mathbf{K}\left(\mathbf{E_e^2}\right) = \textstyle\sum_{e=1}^{N_2} \mathbf{K_e}\left(\mathbf{E_e^2}\right) \\
&\qquad \overline{\Omega_1} \;\; and \;\; \overline{\Omega_2} \;\; connected
\end{aligned}
\tag{2}
$$

From eq. 2, it can be observed that the only requirements on the two domains $\overline{\Omega_1}$ and $\overline{\Omega_2}$ is that their union is equal to the union of Ω_1 and Ω_2 and that their intersection is a null set. The division of the common part of the domain is not given and the solution algorithm can allocate the common part of the domain during the optimization process. As a consequence, the geometries of the two domains $\overline{\Omega_1}$ and $\overline{\Omega_2}$ are not fixed but can change during the optimization. The allocation of the elements of the common domain to one or the other body is controlled by the local sensitivities of each element. Each element is assigned to the domain where it can give the greater contribution to the reduction of the global compliance of the system.

This situation is very different with respect to the usual framework of the density-based topology optimization, where the design domain (and thus the mesh) is fixed (Bendsøe and Sigmund (2004)). Although this fundamental difference, the solution approach proposed in the paper is based on the classical problem of the optimal material distribution by means of the definition of the pseudo-density field and the SIMP method (Bendsøe and Sigmund (2004); Rozvany (2009)). In other words, after identifying the proper division of the domains $\overline{\Omega_1}$ and $\overline{\Omega_2}$, the common SIMP method is employed for optimizing the material distributions in each domain. In this way, promptly available algorithms for the solution of a wide variety of problems can be adapted to the considered problem.

The solution algorithm is depicted in the diagram of Fig. 2. The algorithm is basically divided in two parts, indicated in the figure by the dashed rectangles labelled **A** and **B**.

Sub-algorithm **A** represents a standard topology optimization algorithm. This sub-algorithm follows the solution of the finite element model of the two bodies

(*block 1* in Fig. 2). Sub-algorithm **B** is the innovative part of the proposed algorithm and has the function of assigning each element of the shared part of the domain (Ω_{1-2}) to one of the two bodies. Following the diagram of Fig. 2, the concurrent optimization algorithm is now described.

3.1 *Block 1*: solve the two FE models on Ω_1 and Ω_2.

The finite element models of the two bodies, with the corresponding properties, loads and constraints, are constructed and solved independently over the two domains Ω_1 and Ω_2. It can be noted that Ω_1 and Ω_2 are the whole domain spaces of the two bodies, including the shared part. By building and solving the finite element models always on the two sets Ω_1 and Ω_2, it is possible to use a fixed mesh for all the optimization process. However, in this way, the elements of the shared set Ω_{1-2} are considered in both models. In the subsequent steps, a procedure to penalize the densities of one of the two bodies on each element of the shared set will be considered. By this penalization, each element actually contributes only to the structural stiffness of one of the two bodies.

3.2 Sub-algorithm **A**: topological optimization over Ω_1 and Ω_2.

This sub-algorithm is a standard topology optimization algorithm employed to compute the pseudo-density field in the two domains. In this paper, the optimization algorithm presented in Sigmund (2001) is used, with the only minor modification consisting in the substitution of the bisection method used to solve the Lagrange multipliers on the density by a Trust-Region Dogleg method (Conn et al. (2000)). The steps of the topology optimization algorithm are the following.

- *Block A1: computation of the sensitivities on Ω_1 and Ω_2.* For each element of Ω_1 and Ω_2, the sensitivities of the total compliance of each element with

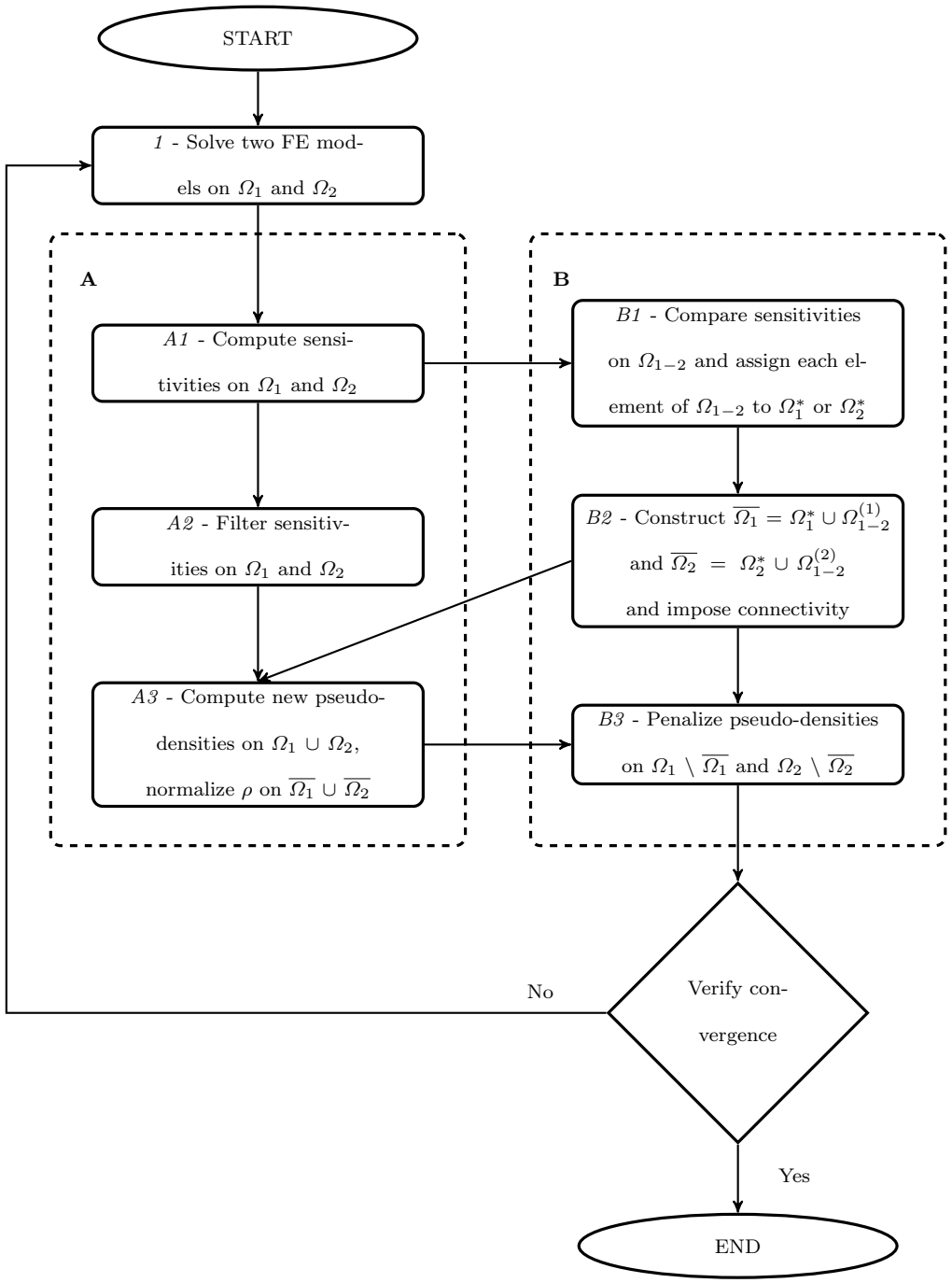

Fig. 2 Diagram of the algorithm for the concurrent topological optimization.

respect to the pseudo-density are computed as (Sigmund (2001))

$$\frac{\partial l}{\partial x_e} = -p\rho\left(x_e\right)^{p-1} \mathbf{u_e^T K_e^* u_e} \tag{3}$$

where l is the total compliance, x_e the location of the element, $\mathbf{u_e}$ the element displacements and $\mathbf{K_e^*}$ the reference stiffness matrix of the element. For the penalization exponent p, a value of 3 is used.

Eq. 3 is computed on all the elements of Ω_1 and Ω_2. This means that the sensitivities of the elements of the shared domain Ω_{1-2} are computed twice, one time with respect to the solution of the finite element model of the first body on Ω_1 and one time with respect to the solution of the finite element model of the second body on Ω_2.

- *Block A2: filtering of the sensitivities on Ω_1 and Ω_2.* As suggested in Sigmund (2001), a filter on the sensitivities is implemented in order to ensure a regular solution. The filter is formulated as (Sigmund (2001))

$$\frac{\widehat{\partial l}}{\partial x_e} = \frac{1}{x_e \sum_{f=1}^{N} \hat{H}_f} \sum_{f=1}^{N} \hat{H}_f x_f \frac{\partial l}{\partial x_f} \tag{4}$$

The weighting factor $\hat{H}_f$ is written as

$$\hat{H}_f = r_{min} - \texttt{dist}\left(e,f\right), \;\; with \;\; \left\{f \in N | \texttt{dist}\left(e,f\right) \leq r_{min}\right\}, \;\; e = 1,...,N \tag{5}$$

where the distance is computed between the centre of the elements e and f. The pseudo-densities are filtered separately on Ω_1 and Ω_2.

- *Computation of the new pseudo-density field on $\Omega_1 \cup \Omega_2$.* The new density field is computed as (Bendsøe and Sigmund (2004); Sigmund (2001))

$$\rho_e^{new} = \begin{cases} \max\left(\rho_{min}, \rho_e - m\right), & if \quad \rho_e B_e^{\eta} \leq \max\left(\rho_{min}, \rho_e - m\right) \\ \rho_e B_e^{\eta}, & if \quad \max\left(\rho_{min}, \rho_e - m\right) < \rho_e B_e^{\eta} < \min\left(1, \rho_e + m\right) \\ \min\left(1, \rho_e + m\right) & if \quad \min\left(1, \rho_e + m\right) \leq \rho_e B_e^{\eta} \end{cases} \tag{6}$$

where m is a positive move limit, ρ_{min} is the minimum pseudo-density for any element to avoid numerical singularities, η is a numerical damping coefficient and B_e represent the optimality condition

$$B_e = \frac{-\frac{\partial l}{\partial x_e}}{\lambda \frac{\partial V}{\partial x_e}} \tag{7}$$

λ is a Lagrange multiplier computed by a Trust-Region Dogleg algorithm (and not by a bisection method as in Sigmund (2001)).

As for the sensitivities, also the new pseudo-density field is computed twice for the elements of Ω_{1-2}.

The computation of the new pseudo-density field is performed on the whole domain $\Omega_1 \cup \Omega_2$. In this way, the total mass is not assigned a priori, but is divided among the two bodies accordingly to the computed sensitivities. To guarantee that the total mass on the two physical domains $\overline{\Omega_1}$ and $\overline{\Omega_2}$ matches the target on the design volume fraction, the Lagrange multiplier λ is computed over $\overline{\Omega_1} \cup \overline{\Omega_2}$ and not $\Omega_1 \cup \Omega_2$.

The output of the sub-algorithm **A** are the new pseudo-densities fields on the two domains Ω_1 and Ω_2.

3.3 Sub-algorithm **B**: computation and enforcement of the connectedness of the two domains $\overline{\Omega_1}$ and $\overline{\Omega_2}$.

Sub-algorithm **B** is devoted to the assignment of each element of the shared part of the design space Ω_{1-2} to either of the two bodies. This assignment is performed accordingly to the relative sensitivity of each element with respect to the total compliance of the two bodies. In other words, each shared element is assigned to the body that provides the higher variation on the compliance. Moreover, this sub-algorithm regularizes the two domains by enforcing the connectedness condition. The sub-algorithm comprises the following steps.

- *Block B1: Comparison of the sensitivities on Ω_{1-2} and assignment of each element of Ω_{1-2} to Ω_1^* or Ω_2^*.* For each element of Ω_{1-2} the two values of the sensitivities computed in *Block A1* are compared. Each element is then assigned to Ω_{1-2}^1 if the sensitivity computed with respect to Ω_1 is greater than the sensitivity computed with respect to Ω_2 or to Ω_{1-2}^2 otherwise.

- *Block B2: Construction of $\overline{\Omega_1} = \Omega_1^* \cup \Omega_{1-2}^{(1)}$ and $\overline{\Omega_2} = \Omega_2^* \cup \Omega_{1-2}^{(2)}$ and connectivity analysis.* The sets Ω_{1-2}^1 and Ω_{1-2}^2 built in the previous step are united with Ω_1^* and Ω_2^* respectively to create the sets $\overline{\Omega_1}$ and $\overline{\Omega_2}$. At this point, the two sets $\overline{\Omega_1}$ and $\overline{\Omega_2}$ have been created exclusively on the basis of the relative sensitivities computed on the elements. There is a high probability that the resulting sets are disconnected and thus not physically admissible.

  An intuitive definition of connectedness in space can be given as follows. A set is said to be connected if two points of the set can be connected by a curve belonging to the set. In this paper, a more restrictive definition of connectedness is used. In fact, by the previous definition, a surface (or a three dimensional

region of space) is considered connected if two parts of the surface have in common just one point. This is not sufficient to have a physical meaning of the structure. We say that to be considered connected, and have a physical meaning, all the elements of the region must share at least one edge in a two dimensional space or a face in a three dimensional space with the rest of the region. By considering this definition, each element of the two sets is analyzed. The elements are grouped according to their connectivity with other elements and the whole region is mapped. Finally, if from this map a part of a region is not connected, it is moved from one set to the other. In this analysis, both domains are treated simultaneously, i.e. the connectivity analysis does not depend on the order on which the two domains are considered.

- *Block B3: Penalization of the pseudo-densities on* $\Omega_1 \setminus \overline{\Omega_1}$ *and* $\Omega_2 \setminus \overline{\Omega_2}$. The new pseudo-density field computed in the block *A3* refers to the whole domain $\Omega_1 \cup \Omega_2$. That is, the elements of Ω_1 but not belonging to $\overline{\Omega_1}$ and of Ω_2 but not belonging to $\overline{\Omega_2}$ have a value of the pseudo-density that depends on their sensitivities and could contribute to the stiffness of the system. To make their contribution vanishing and avoid singularities in the stiffness matrices of the two systems, the pseudo-densities of these elements (belonging to the two sets $\Omega_1 \setminus \overline{\Omega_1}$ and $\Omega_2 \setminus \overline{\Omega_2}$) are multiplied by a penalization factor fixed to 0.05. In any case, the minimum pseudo-density of any element is ρ_{min}.

The outputs of the sub-algorithm **B** are the two pseudo-density fields on Ω_1 and Ω_2, where the elements of $\Omega_1 \setminus \overline{\Omega_1}$ and $\Omega_2 \setminus \overline{\Omega_2}$ have been penalized in order to make their contribution negligible, and the maps of the two sets $\overline{\Omega_1}$ and $\overline{\Omega_2}$.

The optimization algorithm is then arrested if the maximum difference on the pseudo-density of the elements is below a certain threshold or if a maximum number of iterations is reached.

4 Numerical examples

In this section, three numerical examples are presented to show the potentialities of the presented approach. The first example refers to a situation in which the shared part of the design domains can be divided in order to obtain, for the two bodies, the known solution to two problems of topology optimization already published in the literature. In the second problem, a quite complex symmetric situation is solved. The problem can test the ability of the method to maintain the symmetry in the solution of the problem. Finally, the third example refers to a three dimensional design problem.

For examples 1 and 2, a mesh of bilinear quadrilateral elements of dimension 1×1 is used. Since the optimization problem is a nonconvex problem, the solution depends on the initial conditions. In the following examples, the initial condition are given by an uniform pseudo-density equal to the required volume fraction for all the elements. The shared domain is initially assigned to both bodies, i.e. $\overline{\Omega_1} = \Omega_1$ and $\overline{\Omega_2} = \Omega_2$ at the first step of the iteration. The minimum pseudo-density is 0.001 and the filter distance ρ_{min} is equal to 1.5 times the characteristic dimension of the elements.

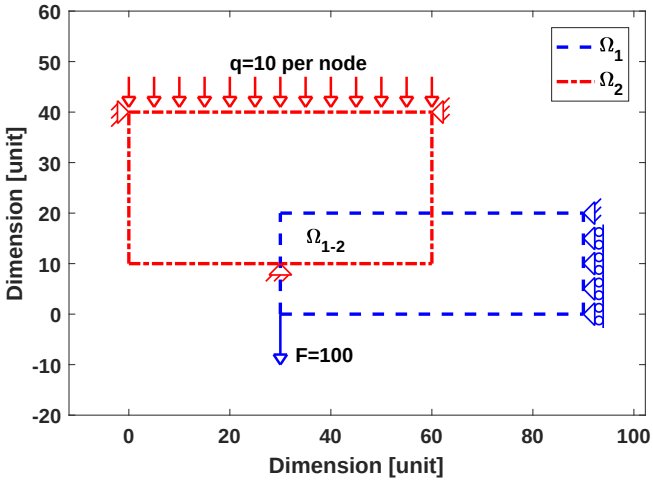

Fig. 3 Example 1. Definition of two optimization problems from the literature. The problem defined over Ω_1 is taken from Bendsøe and Sigmund (2004) at pag. 49. The problem defined over Ω_2 is taken from Buhl (2002) at pag. 342.

4.1 Example 1: literature cases

In this example two problems, whose optimal solution is known from the literature, are considered. The two domains of the problems are overlapped in such a way that the shared part of the domains can be divided in order to obtain for both problems the optimal solution. The example is depicted in Fig. 3. The problem corresponding to the domain Ω_1 is the very well known problem of the cantilever with an end load (see for instance Bendsøe and Sigmund (2004) pag. 49). The second problem, defined on Ω_2 is a three support structure loaded with a distributed load presented in Buhl (2002) at pag. 342. The overall volume fraction is 0.4.

In Fig. 4 the results of the concurrent topological optimization are shown. In Fig. 4A, the division of the common part of the design space is reported and in Fig. 4B the two optimized structures can be seen. The two optimized structures

correspond to the optimal solutions reported in the literature. In particular, the cantilever is actually the well known solution of the problem. The solution of the three supports structure is very close to the solution reported in Buhl (2002). The small differences are due to a very different mesh size, volume fraction and filter settings.

According to the division of the domains of Fig. 4A, the domain $\overline{\Omega_1}$ has 1112 elements, while the domain $\overline{\Omega_2}$ 1588. The volume fractions are respectively 0.53 (corresponding to 591.5 units of mass) and 0.31 (corresponding to 488.5 units of mass). The overall volume fraction is 0.4 as set as target and corresponding to 1080 units of mass over the 2700 elements corresponding at $\overline{\Omega_1} \cup \overline{\Omega_2}$.

Referring to the division of the design space, it can be observed that the design space is divided in a way which allows the optimal material distributions of the two structures (Fig 4A). The obtained design space division is not intuitive without any a priori knowledge of the solution. In Fig. 5 the results for the optimization of the problem of Fig. 3 are reported for four reasonable a priori divisions of the design space. In absence of any other information, four division of the design space are considered, namely:

- All of the common design Ω_{1-2} space is attributed to Ω_1, so that $\overline{\Omega_1} = \Omega_1$.
- All of the common design Ω_{1-2} space is attributed to Ω_2, so that $\overline{\Omega_2} = \Omega_2$.
- Each element of the common design Ω_{1-2} space is attributed to the closest domain.
- The common design Ω_{1-2} space is divided in half along the diagonal and each half of the common domain is attributed to the closest domain.

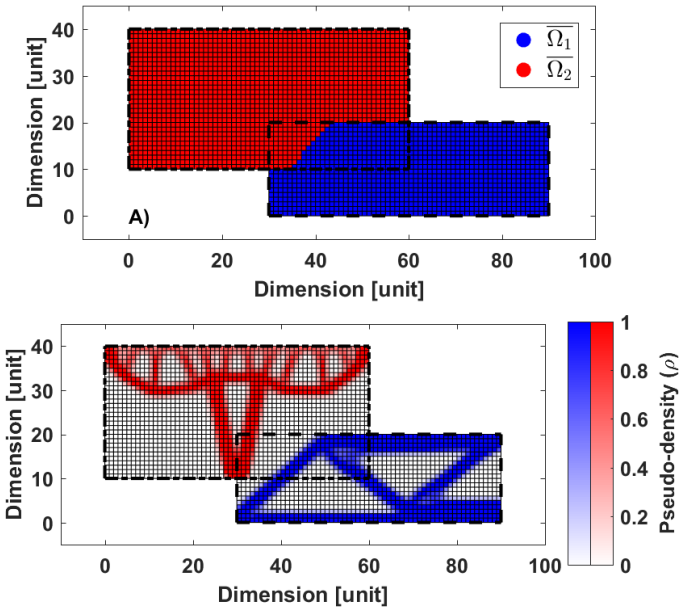

Fig. 4 Example 1. Solution of two optimization problems from the literature. The obtained solutions correspond to the solutions reported in the literature (see Bendsøe and Sigmund (2004) at pag. 49 and Buhl (2002) at pag. 342). A): division of the design space. B): optimized structures.

The four described divisions are depicted on the left column of Fig. 5. On the right side of Fig. 5 the four corresponding solutions are depicted. The compliances of the structures obatained on the two domains Ω_1 and Ω_2 in the four conditions are shown in Fig. 6. It can be seen that the solution obtained by the concurrent topological optimization algorithm is always dominating the other solutions, having the minimum value of both the compliances. It is interesting to note that the optimal solution has lower compliance of the division $\overline{\Omega_1} = \Omega_1$ on Ω_1 and of the division $\overline{\Omega_2} = \Omega_2$ on Ω_2 even if these divisions can have the optimal material distributions on those domains. This is due to the mass repartition according to the

Table 1 Results of the optimization problem of Fig. 3.

Common domain division	Mass on Ω_1	Mass on Ω_2	Compliance on Ω_1	Compliance on Ω_2	Total compliance
Optimal solution	591.5	488.5	$8.36 \cdot 10^6$	$5.66 \cdot 10^6$	$14.01 \cdot 10^6$
$\overline{\Omega_1} = \Omega_1$	581.0	499.0	$8.50 \cdot 10^6$	$7.13 \cdot 10^6$	$15.62 \cdot 10^6$
$\overline{\Omega_2} = \Omega_2$	595.4	484.6	$13.30 \cdot 10^6$	$5.74 \cdot 10^6$	$19.04 \cdot 10^6$
Minimum distance	592.9	487.1	$8.67 \cdot 10^6$	$6.76 \cdot 10^6$	$15.43 \cdot 10^6$
Diagonal	592.8	487.2	$8.41 \cdot 10^6$	$6.74 \cdot 10^6$	$15.15 \cdot 10^6$

sensitivities (*Block A3* in Sect. 3) which redistributes the mass in order to reduce the total compliance. In other words, the algorithm assigns a higher value of mass, with respect to the optimal solution, to the domain in which the optimal material distribution cannot be achieved in order to compensate for the less efficiency of the obtained material distribution (see table 1).

4.2 Example 2: symmetric structure

The considered example is shown in Fig. 7. This example consists of two identical structures rotated of 180^o. Each structure is a cantilever with a fixed end and two forces applied to one corner of the opposite end. The corner where the forces are applied has been chosen in order to have the application points inside the shared part of the domain.

In Fig. 8, the results of the optimization process are depicted. The obtained solution, despite its high level of complexity, shows a very good symmetry. In fact, by analysing Fig. 8, it can be observed that the two structures are actually the same structure rotated of 180^o. The compliances computed for the two bodies differ of about 0.01% and the mass is the same up to round off error.

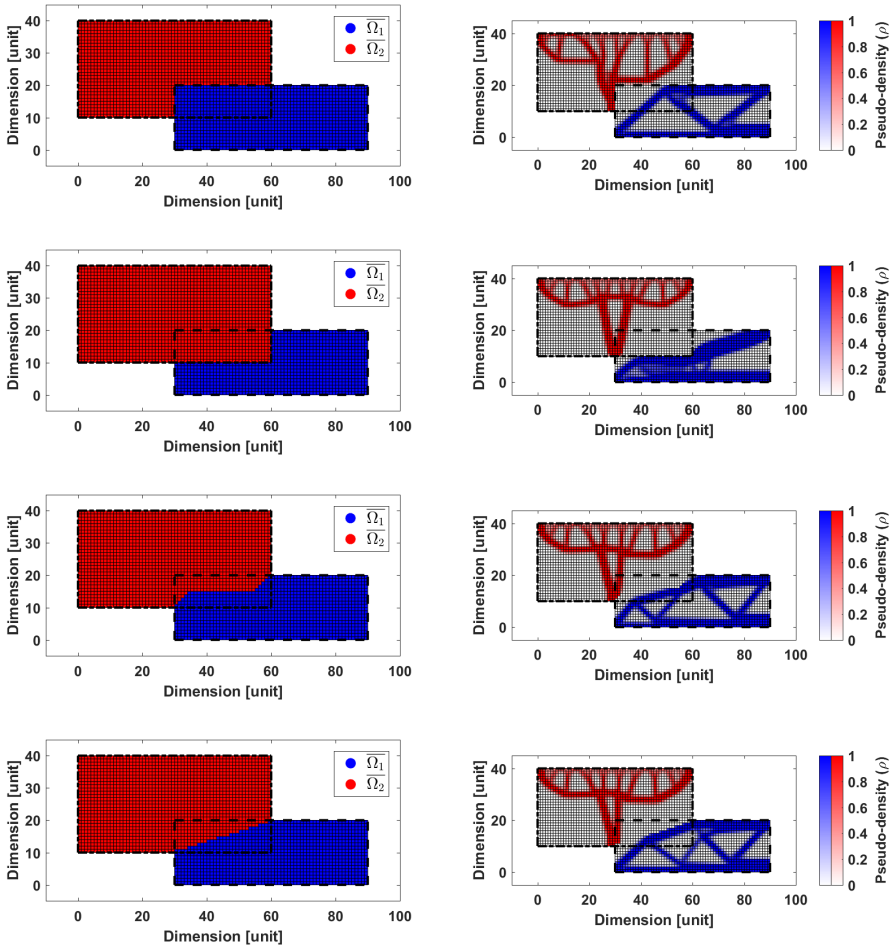

Fig. 5 Example 1. Solutions to the problem of Fig. 3 for four reasonable a priori divisions of the common domain Ω_{1-2}. From top to bottom: $\overline{\Omega_1} = \Omega_1$, $\overline{\Omega_2} = \Omega_2$, division by the minimum distance, division along the diagonal. Left: divisions of the design space. Right: optimized structures.

By inspecting Fig. 8 bottom, it can be noted that a small almost void band is present between the two bodies. This almost void is due to the filter on the sensitivities (step *A2* in Fig.2). In fact, in case a element with pseudodensity close to one is close to the border of the assigned domain, the filter smooths the

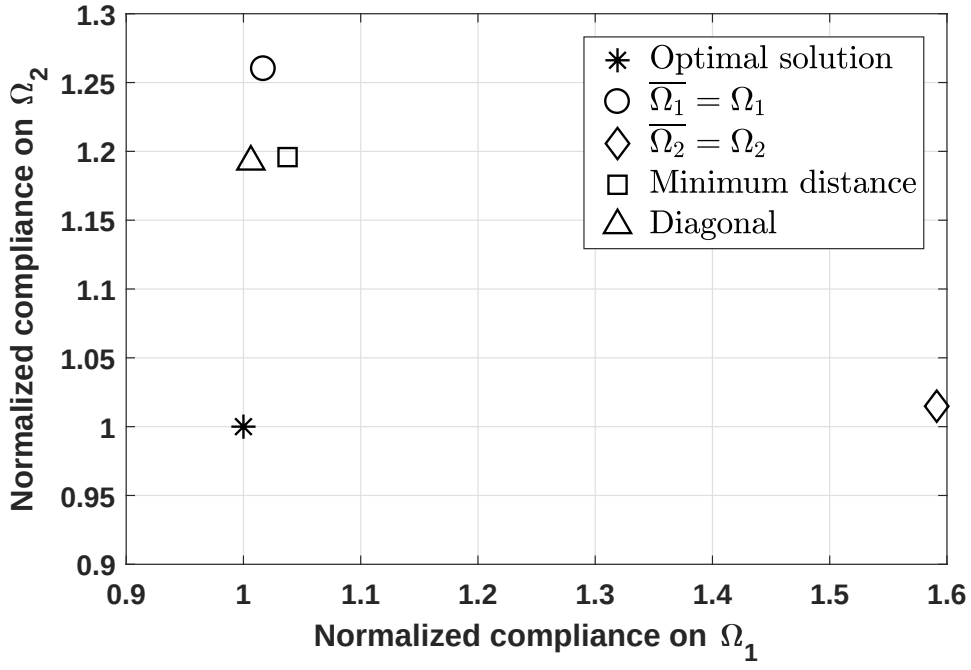

Fig. 6 Example 1. Comparison of the normalized compliances of the two structures obtained by the optimal solution of the concurrent topological optimization algorithm and by considering four reasonable a priori divisions of the common domain Ω_{1-2} ($\overline{\Omega_1} = \Omega_1$, $\overline{\Omega_2} = \Omega_2$, division by the minimum distance, division along the diagonal).

transition of the density to the almost zero of the neightbour elements. In case the two resulting structures are too close and could touch after deformation, an effect which is not modeled, the parameters of the filter could be used to allow for a certain amount of clearance.

4.3 Example 3: wheel and brake caliper assembly

In this subsection, the described method is used for the optimization of a wheel and brake caliper assembly. The example refers to a complex 3D structure and it

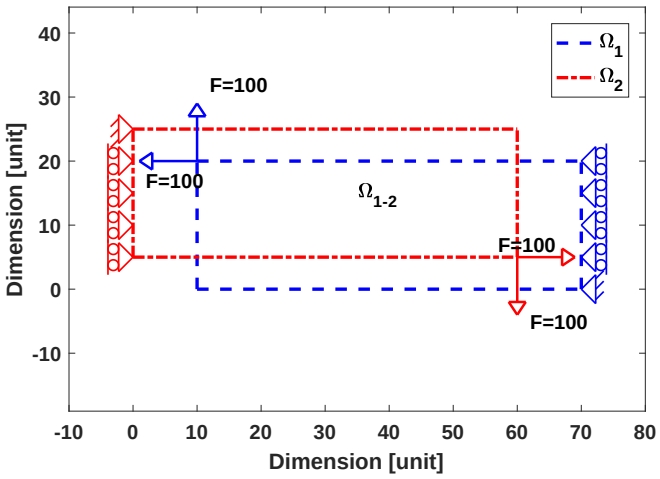

Fig. 7 Example 2. Definition of two optimization problems rotated of 180^o. Each problem is a cantilever with a fixed end and two forces applied to one corner of the opposite end. Notice that the forces are applied inside the shared part of the domains.

is solved by using a commercial finite element software (Abaqus^{TM}2016). The example demonstrates the possibility to apply the optimization algorithm presented in this paper to a commercial software to solve practical 3D problems.

The wheel and brake caliper are depicted in Fig. 9. The caliper is a fixed caliper with three pistons per each side. The caliper is constrained to the ground at the location of the two radial holes in the inner side of the caliper. To the caliper, a pressure load of is 6.3 MPa at each piston location and a force of 10 kN on each of the two stops of the pads in the circumferential direction is applied.

Referring to the wheel, four different load cases have been considered. For each load case, the inner side of the wheel hub is constrained to the ground and a pressure of 0.1 MPa is applied to the rim. The load is applied to a reference point corresponding to the centre of the contact patch and connected to the two sides

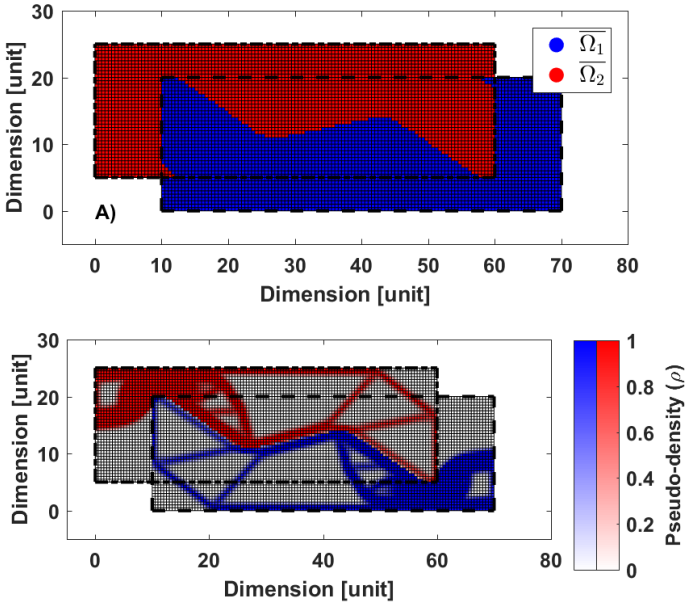

Fig. 8 Example 2. Solution of two optimization problems rotated of 180^o. A): division of the design space. B): optimized structures.

of the flange of the ring for a angle of 72°. The four load cases are described in table 2.

The two models are meshed by trilinear brick elements with reduced integration and solved by a linear solver. For the caliper, 23157 elements have been used, while for the wheel 206640 elements.

In Fig. 10, the wheel and brake caliper assembly is shown and the design space and the non design space are reported. In the picture, only half of the wheel is reported to show the brake caliper model. For both components, the design space is divided into the non shared part (region that is assigned exclusively to one component) and into the shared part (region that can be assigned to either com-

Table 2 Loads applied to the wheel in the four considered load cases.

Load case	Vertical force [N]	Longitudinal force [N]	Lateral force [N]
Bump	15000	7500	0
Corner	7000	0	7000
Straight brake	7000	7000	0
Corner brake	8000	5500	5000

ponent during the optimization process). The non design domains are reported in red, while the design domains are reported in blue (non shared parts) and in white (shared parts). It must be observed that since the wheel rotates with respect to the caliper, a complete annular section of the wheel has to be considered as shared domain and not only the part corresponding to the actual position of the caliper. Moreover, when dividing the shared part of the domains, a cylindrical symmetry condition must be considered. The cylindrical symmetry condition is applied as follows. The meshes have been realized along cylindrical paths. In this way, the elements of the shared domain pertaining to each of the two bodies can be grouped according to the circumferential path on which have been generated. The sensitivity of all the elements pertaining to the same circumferential group is summed up and the comparison is realized per groups between the two bodies. Once a circumferential group is assigned to one of the two bodies, the pseudodensity of the elements of the group is computed in the standard way, i.e. the elements of the same group can have different pseudodensities.

Finally, in the optimization of the wheel, in order to obtain a reasonable material distribution, a cyclic symmetry with the repetition of five sectors is applied.

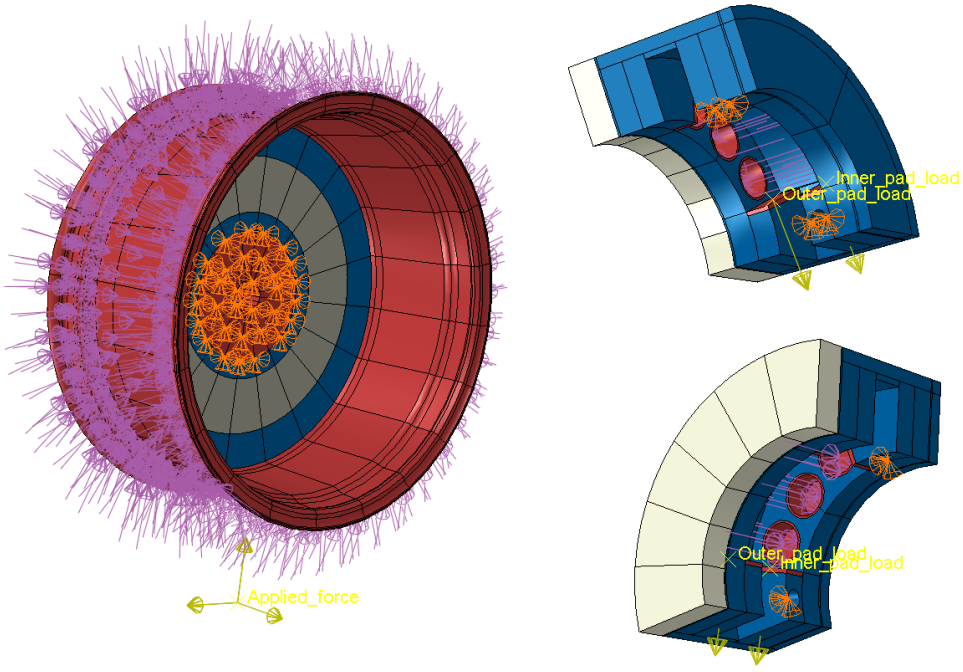

Fig. 9 Wheel and brake caliper models. Left wheel. Right: caliper views.

The resulting wheel will be a periodic structure with the repetition of five sectors of 72^{o} each. No manufacturability constraint is considered.

The optimization problem is solved by using Abaqus^{TM}2016 for the solution of the finite element model and a handwritten code to read the results, implement the optimization algorithm and write the new input file. The handwritten code is realized by using Python and Matlab^{TM}.

The results of the optimization process, with a overall target volume fraction of 0.5, is shown in Fig. 11 and Fig. 12. Fig. 11 shows the assignment of the shared part of the domain, while Fig. 12 shows the optimized material distribution removing all the elements with pseudodensity lower than 0.5. The obtained volume fractions for the two bodies are 0.431 and 0.516 for the brake caliper and wheel respectively.

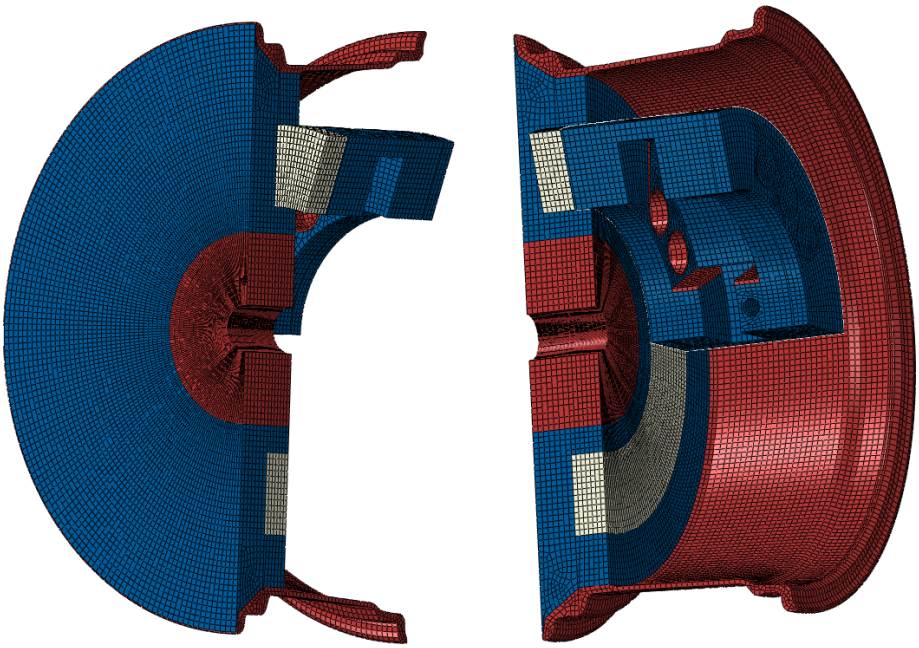

Fig. 10 Wheel and brake caliper assembly. Red: non design domains. Blue: non shared parts of the design domain. White: shared part of the design domain. Only half of the wheel is depicted. Notice that given the rotation of the wheel, the shared part of the design domain has two different geometries for the two bodies.

In table 3 the results of the optimization of the wheel and brake caliper assembly for different divisions of the shared part of the domain are reported. The considered divisions are the optimal one, the shared domain assigned completely to the wheel and the shared domain assigned completely to the brake caliper. From table 3, it can be observed that the optimal division shows a lower level of compliance of the other two divisions. Moreover, as found for Example 1 in Sec. 4.1, not only the optimal solution has the lowest total compliance, but also the lowest values for the compliances of each of the two bodies. This shows that also in

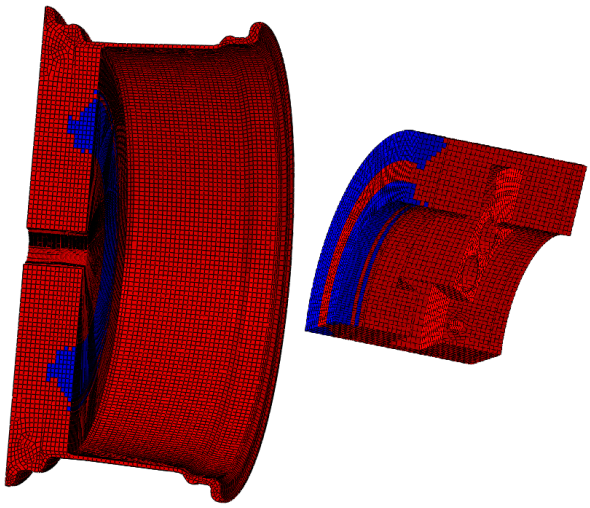

Fig. 11 Optimization results - division of the design space. Red: elements of Ω_i and belonging to $\overline{\Omega_i}$ (with $i = 1, 2$). Blue: elements of Ω_i but not belonging to $\overline{\Omega_i}$ (with $i = 1, 2$). Left: wheel. Right: brake caliper.

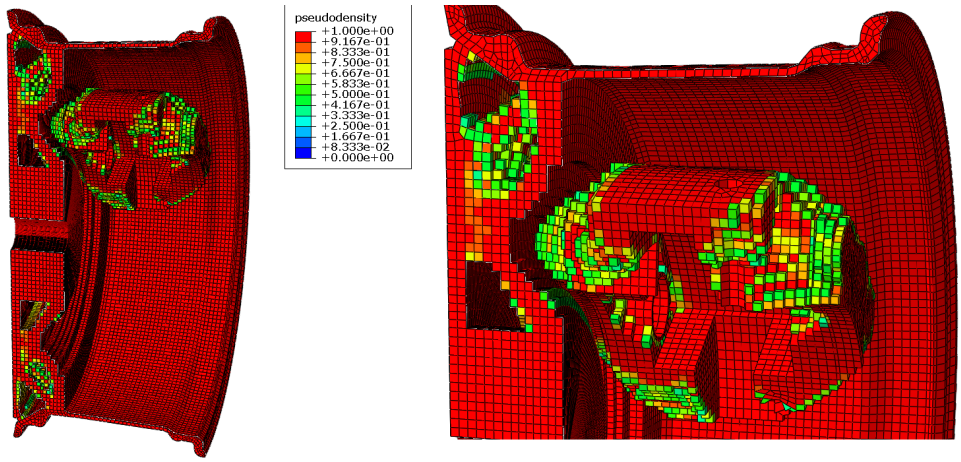

Fig. 12 Results of the optimization of the wheel and brake caliper assembly. The elements with pseudodensity lower than 0.5 have been removed.

Table 3 Results of the optimization of the wheel and brake caliper assembly with different divisions of the shared domain.

Shared domain division	% of mass on brake caliper	% of mass on wheel	Brake caliper compliance*	Wheel compliance*	Total compliance*
Optimal solution	16.8	83.2	0.256	0.744	1.000
Shared domain assigned wheel	18.0	82.0	0.455	0.682	1.137
Shared domain assigned brake caliper	16.2	83.8	0.257	1.202	1.459

* normalized with respect to the total compliance of the "Optimal solution".

this complex three-dimensional problem the proposed algorithm is able to identify an effective division of the domain.

Fig. 13 shows the evolution of some relevant variables during the optimization problem. As expected, the greater variation of the variables is in the first few cycles and then a convergence configuration is reached. From the figure, it can be observed that for each body both mass and vary during the optimization process, while the overall volume fraction is constant.

5 Conclusion

In the present paper a novel topological optimization problem has been presented. The problem refers to the concurrent topological optimization of two structures sharing part of the design domain. This kind of problem is of interest in systems design where more than one body has to be considered.

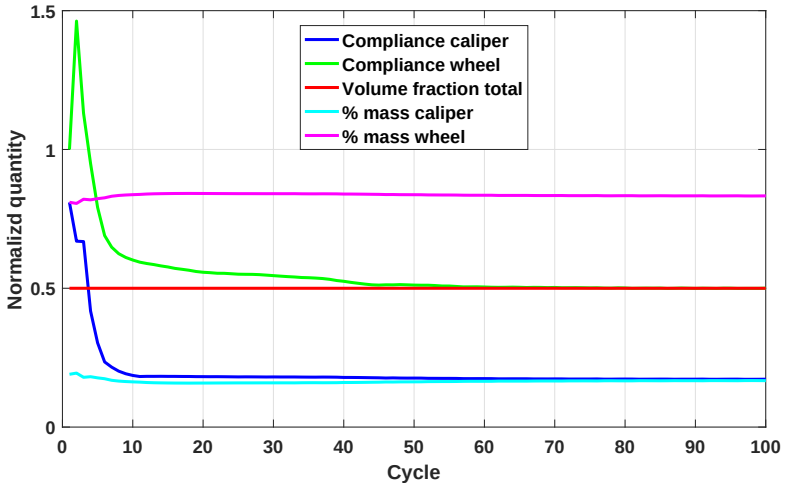

Fig. 13 Evolution of relevant variables during the optimization process.

In the paper, an algorithm based on the SIMP approach for the solution of this kind of problems is proposed. The main objective has been the derivation of an algorithm for the numerical solution of the problem that could be considered as an add on to current topological optimization algorithms.

The proposed algorithm assigns the shared space to one or the other body depending on the relative sensitivity to each element to the total compliance of the system. After each element has been assigned to one of the two design domains, the connectedness of the two domains is checked. In case some unconnected regions are present, the assignment of these regions is reversed and the connectedness of each of the two domains is enforced. The volume fraction is enforced at system level, i.e. the volume fractions of the two domains can be different, but the total volume fraction complies with the set value. In this way, the available mass can be allocated in the most convenient way among the two bodies.

By considering three examples, two in two dimensions and one real world three dimensional problems, the algorithm has proved to be actually able to solve the proposed problem. In particular, the last example has shown the practical interest of this kind of problems. The algorithm has been used with a commercial finite element software by considering a SIMP approach and a cyclic symmetry in the solution, proving the applicability of the method with existing optimization algorithm. Further developments of the method should consider the possibility to mesh independently, i.e. with different element sizes and types, the two bodies to allow for the solution of assemblies with more complex geometries. Also, the possibility to include contact interactions in the shared part of the domain will be investigated.

References

Martin P. Bendsøe and Ole Sigmund. *Topology optimization. Theory, methods, and applications.* Springer Berlin Heidelberg, Berlin, Heidelberg, 2nd edition, 2004. ISBN 978-3-642-07698-5. doi: 10.1007/978-3-662-05086-6. URL `http://link.springer.com/10.1007/978-3-662-05086-6`.

T. Buhl. Simultaneous topology optimization of structure and supports. *Structural and Multidisciplinary Optimization*, 23(5):336–346, 2002. ISSN 1615147X. doi: 10.1007/s00158-002-0194-2.

Anders Clausen, Niels Aage, and Ole Sigmund. Topology optimization with flexible void area. *Structural and Multidisciplinary Optimization*, 50(6):927–943, 2014. ISSN 16151488. doi: 10.1007/s00158-014-1109-8.

A. R. Conn, N. I. M. Gould, and Ph. L. Toint. *Trust Region Methods*. MPS/SIAM Series on Optimization, Society for Industrial and Applied Mathematics, 2000. ISBN 9780898714609.

Hans A Eschenauer and Niels Olhoff. Topology optimization of continuum structures: A review. *Applied Mechanics Reviews*, 54 (4):331, 2001. ISSN 00036900. doi: 10.1115/1.1388075. URL http://appliedmechanicsreviews.asmedigitalcollection.asme.org/article.aspx?articleid=1396619.

Xu Guo and Geng-Dong Cheng. Recent development in structural design and optimization. *Acta Mechanica Sinica*, 26(6):807–823, 2010. ISSN 0567-7718. doi: 10.1007/s10409-010-0395-7. URL http://link.springer.com/10.1007/s10409-010-0395-7.

Matthew Lawry and Kurt Maute. Level set shape and topology optimization of finite strain bilateral contact problems. *International Journal for Numerical Methods in Engineering*, 113(8):1340–1369, 2018. ISSN 10970207. doi: 10.1002/nme.5582.

Zhen Luo, Liyong Tong, Junzhao Luo, Peng Wei, and Michael Yu Wang. Design of piezoelectric actuators using a multiphase level set method of piecewise constants. *Journal of Computational Physics*, 228(7):2643–2659, apr 2009. ISSN 0021-9991. doi: 10.1016/J.JCP.2008.12.019. URL https://www.sciencedirect.com/science/article/pii/S0021999108006633.

Yulin Mei and Xiaoming Wang. A level set method for structural topology optimization and its applications. *Advances in Engineering Software*, 35(7):415–441, jul 2004. ISSN 0965-9978. doi: 10.1016/J.ADVENGSOFT.2004.06.004. URL https://www.sciencedirect.com/science/article/pii/S0965997804000705.

Zhongyan Qian and G. K. Ananthasuresh. Optimal embedding of rigid objects in the topology design of structures. *Mechanics Based Design of Structures and Machines*, 32(2):165–193, 2004. ISSN 15397734. doi: 10.1081/SME-120030555.

G. I. N. Rozvany. A critical review of established methods of structural topology optimization. *Structural and Multidisciplinary Optimization*, 37(3): 217–237, 2009. ISSN 1615-147X. doi: 10.1007/s00158-007-0217-0. URL `http://link.springer.com/10.1007/s00158-007-0217-0`.

O. Sigmund. A 99 line topology optimization code written in matlab. *Structural and Multidisciplinary Optimization*, 21(2):120–127, 2001. ISSN 1615147X. doi: 10.1007/s001580050176.

N Strömberg. Topology optimization of orthotropic elastic design domains with mortar contact conditions. In Maute K Schumacher A, Vietor T, Fiebig S, Bletzinger K-U, editor, *Advances in Structural and Multidisciplinary Optimization: Proceedings of the 12th World Congress of Structural and Multidisciplinary Optimization*, pages 1427–1438, Braunschweig, Germany, 2018. Springer International Publishing. ISBN 978-3-319-67987-7. doi: 10.1007/978-3-319-67988-4. URL `http://link.springer.com/10.1007/978-3-319-67988-4`.

Rouhollah Tavakoli and Seyyed Mohammad Mohseni. Alternating active-phase algorithm for multimaterial topology optimization problems: A 115-line MATLAB implementation. *Structural and Multidisciplinary Optimization*, 49(4):621–642, 2014. ISSN 16151488. doi: 10.1007/s00158-013-0999-1.

Panagiotis Vogiatzis, Shikui Chen, Xiao Wang, Tiantian Li, and Lifeng Wang. Topology optimization of multi-material negative Poisson's ratio metamaterials using a reconciled level set method. *Computer-Aided Design*, 83:15–32, feb 2017. ISSN 0010-4485. doi: 10.1016/J.CAD.2016.09.009. URL

https://www.sciencedirect.com/science/article/pii/S0010448516301154.

Michael Yu Wang and Xiaoming Wang. Color level sets: a multi-phase method for structural topology optimization with multiple materials. *Computer Methods in Applied Mechanics and Engineering*, 193(6-8):469–496, feb 2004. ISSN 0045-7825. doi: 10.1016/J.CMA.2003.10.008. URL https://www.sciencedirect.com/science/article/pii/S0045782503005644.

Yiqiang Wang, Zhen Luo, Xiaopeng Zhang, and Zhan Kang. Topological design of compliant smart structures with embedded movable actuators. *Smart Materials and Structures*, 23(4), 2014. ISSN 1361665X. doi: 10.1088/0964-1726/23/4/045024.

Yu Wang, Zhen Luo, Nong Zhang, and Tao Wu. Topological design for mechanical metamaterials using a multiphase level set method. *Structural and Multidisciplinary Optimization*, 54(4):937–952, 2016. ISSN 16151488. doi: 10.1007/s00158-016-1458-6. URL http://dx.doi.org/10.1007/s00158-016-1458-6.

Yu Wang, Jie Gao, Zhen Luo, Terry Brown, and Nong Zhang. Level-set topology optimization for multimaterial and multifunctional mechanical metamaterials. *Engineering Optimization*, 49(1):22–42, 2017. ISSN 10290273. doi: 10.1080/0305215X.2016.1164853. URL https://doi.org/10.1080/0305215X.2016.1164853.

Liang Xia, Jihong Zhu, Weihong Zhang, and Piotr Breitkopf. An implicit model for the integrated optimization of component layout and structure topology. *Computer Methods in Applied Mechanics and Engineering*, 257: 87–102, apr 2013. ISSN 0045-7825. doi: 10.1016/J.CMA.2013.01.008. URL https://www.sciencedirect.com/science/article/pii/S0045782513000194.

Qiao Zhang, Weihong Zhang, Jihong Zhu, and Tong Gao. Layout optimization of multi-component structures under static loads and random excitations. *Engineering Structures*, 43:120–128, oct 2012. ISSN 0141-0296. doi: 10.1016/J.ENGSTRUCT.2012.05.013. URL https://www.sciencedirect.com/science/article/pii/S0141029612002490.

Weihong Zhang, Jihong Zhu, and Tong Gao. *Topology optimization in engineering structure design*. Elsevier, Oxford, 2016a. ISBN 9781785482243.

Weisheng Zhang, Wenliang Zhong, and Xu Guo. Explicit layout control in optimal design of structural systems with multiple embedding components. *Computer Methods in Applied Mechanics and Engineering*, 290:290–313, jun 2015. ISSN 0045-7825. doi: 10.1016/J.CMA.2015.03.007. URL https://www.sciencedirect.com/science/article/pii/S0045782515001097.

Weisheng Zhang, Jie Yuan, Jian Zhang, and Xu Guo. A new topology optimization approach based on Moving Morphable Components (MMC) and the ersatz material model. *Structural and Multidisciplinary Optimization*, 53(6): 1243–1260, 2016b. ISSN 16151488. doi: 10.1007/s00158-015-1372-3. URL http://dx.doi.org/10.1007/s00158-015-1372-3.

Ji-Hong Zhu, Wei-Hong Zhang, and Liang Xia. Topology Optimization in Aircraft and Aerospace Structures Design. *Archives of Computational Methods in Engineering*, 23(4):595–622, 2016. ISSN 1134-3060. doi: 10.1007/s11831-015-9151-2. URL http://link.springer.com/10.1007/s11831-015-9151-2.